

HOSTED BY



ELSEVIER

<http://ppr.buaa.edu.cn/>

## Propulsion and Power Research

[www.sciencedirect.com](http://www.sciencedirect.com)

## ORIGINAL ARTICLE

# Heat and mass transfer effects on MHD viscoelastic fluid over a stretching sheet through porous medium in presence of chemical reaction

Manoj Kumar Nayak<sup>a,\*</sup>, Gauranga Charan Dash<sup>b</sup>, Lambodar Prasad Singh<sup>c</sup><sup>a</sup>*Department of Physics, Radhakrishna Institute of Technology and Engineering, Bijupatnaik University of Technology, Odisha, India*<sup>b</sup>*Department of Mathematics, I.T.E.R., Siksha 'O' Anusandhan University, Odisha, India*<sup>c</sup>*Department of Physics, Utkal University, Odisha, India*

Received 19 November 2014; accepted 5 May 2015

Available online 19 February 2016

**KEYWORDS**Stretching sheet;  
Porous medium;  
Viscoelastic;  
Chemical reaction;  
Kummer's function

**Abstract** An attempt has been made to study the heat and mass transfer effects in a boundary layer flow through porous medium of an electrically conducting viscoelastic fluid subject to transverse magnetic field in the presence of heat source/sink and chemical reaction. It has been considered the effects of radiation, viscous and Joule dissipations and internal heat generation/absorption. Closed form solutions for the boundary layer equations of viscoelastic, second-grade and Walters'  $B'$  fluid models are obtained. The method of solution involves similarity transformation. The transformed equations of thermal and mass transport are solved by applying Kummer's function. The solutions of temperature field for both prescribed surface temperature (PST) as well as prescribed surface heat flux (PHF) are obtained. It is important to remark that the interaction of magnetic field is found to be counterproductive in enhancing velocity and concentration distribution whereas the presence of chemical reaction as well as porous matrix with moderate values of magnetic parameter reduces the temperature and concentration fields at all points of flow domain.

© 2016 National Laboratory for Aeronautics and Astronautics. Production and hosting by Elsevier B.V.

This is an open access article under the CC BY-NC-ND license

[\(http://creativecommons.org/licenses/by-nc-nd/4.0/\)](http://creativecommons.org/licenses/by-nc-nd/4.0/).

## 1. Introduction

The importance of fluid flow over a stretching sheet can be perceived for its ever increasing inevitable applications in industries and in contemporary technology. The applications

\*Corresponding author. Tel.: +91 9040555158.

E-mail address: mnkec1973@gmail.com (Manoj Kumar Nayak).

Peer review under responsibility of National Laboratory for Aeronautics and Astronautics, China.

**Nomenclature**

$K_p$	permeability parameter
$k$	thermal conductivity
$M_n$	magnetic parameter
$R_c$	viscoelastic parameter
$B_0$	magnetic field strength
$Pr$	Prandtl number
$Q$	heat source/sink parameter
$Sc$	Schmidt number
$T'$	temperature of the field
$T$	non-dimensional temperature
$p$	pressure
$t$	non-dimensional time
$D$	molecular diffusivity
$q_r$	radiative heat flux
$\nu$	kinematics viscosity
$C_p$	specific heat
$R$	radiation parameter

$q_w$	wall heat flux
$Ec$	Eckert number
$\tau_w$	wall shear stress
$C_f$	skin friction coefficient
$T_\infty$	temperature far from sheet
$k_0$	modulus of the viscoelastic fluid
$T_w$	wall temperature
$m_w$	rate of mass flux
$K_c$	chemical reaction parameter
$k_1$	mean absorption coefficient
$A, B, E_0, E_1$	constants

**Greek letters**

$\alpha$	thermal diffusivity
$\rho$	density of the fluid
$\sigma^*$	Stefan–Boltzmann constant
$\sigma$	electrical conductivity

of the stretching sheet problem are such as polymer sheet extrusion from a dye, drawing, thinning and annealing of copper wires, glass fiber and paper production, the cooling of a metallic plate in a cooling bath etc. The production of these sheets requires that the melt issues from a slit and is stretched to get the desired thickness. The final product depends on rate of cooling in the process and the process of stretching. Sakiadis [1] was first to study the boundary-layer behavior on a continuous solid surface moving with constant speed. Crane [2] was the first to achieve an elegant analytical solution to the boundary layer equations for the problem of steady two-dimensional flow through a stretching surface in a quiescent incompressible fluid.

The growing need for chemical reaction and hydrometallurgical industries needs the study of heat and mass transfer with chemical reaction. There are numerous transport processes that are governed by the combined action of buoyancy forces due to both thermal and mass diffusion in the presence of chemical reaction effect. These processes occur in the nuclear reactor safety and combustion systems, solar collectors, metallurgical and chemical engineering etc.

Khan and Sanjayanand [3] reported an analytical solution of the viscoelastic boundary layer flow and heat transfer over an exponentially stretched sheet considering the viscous dissipation in the heat transport equation. Kar et al. [4] investigated the heat and mass transfer effects on a dissipative and radiative viscoelastic magnetohydrodynamic (MHD) flow over a stretching porous sheet.

Mushtaq et al. [5] examined the effects of thermal buoyancy on viscoelastic flow of a second grade fluid past a vertical stretching sheet. They have considered local non-similarity method and Kellor box scheme to solve the resulting equation. Further, Arnold et al. [6] have studied the viscoelastic fluid flow and heat transfer characteristics over a stretching sheet taking into account the effects of frictional heating and internal heat

generation/absorption. Bataller [7] investigated the effect of thermal radiation on heat transfer in a boundary layer viscoelastic second order fluid over a stretching sheet with internal heat source/sink. Recently, Hayat et al. [8] studied the effects of chemical reaction of unsteady three dimensional flow of couple stress fluid over a stretching surface. Gireesha et al. [9] have studied the boundary-layer flow and heat transfer of a dusty fluid flow over a stretching sheet in presence of non-uniform heat source/sink and radiation. Parsa et al. [10] investigated the MHD boundary-layer flow over a stretching surface with internal heat generation or absorption. Gupta and Gupta [11] have investigated heat and mass transfer in hydrodynamic fluid flow over an isothermal stretching sheet with suction/blowing effects. Vajravelu and Rollins [12] have studied the flow and heat transfer introducing the temperature dependent heat source and sink. But these studies are confined to hydrodynamic flow and heat transfer in Newtonian fluids. However, most of the practical situations demand for fluids those are non-Newtonian in nature which are extensively used in many industrial and engineering applications.

Raptis [13] studied the heat transfer in a viscous fluid over a stretching sheet with viscous dissipation with and without porous medium. Mahapatra and Gupta [14] also discussed stagnation-point flow of a viscoelastic fluid towards a stretching surface. Cortell [15] has worked on viscous flow and heat transfer over a nonlinearly stretching sheet. Effect of viscous dissipation and radiation on the thermal boundary layer over a nonlinearly stretching sheet was also studied by Cortell [16].

Singh [17] and Chen [18] contributed recently to this field of study. All their works are related to viscoelastic fluid model in the presence of magnetic field. They considered either an oscillatory stretching surface or surface with a linearly varying velocity. They have used hypergeometric function i.e., Kummer's function. All these works reported above considered either radiation effect/viscous

dissipation or both. The novelty of the present study is starred due to the following three aspects.

- (i) Inclusion of porous media is justified since the flow and heat transport processes occur by using insulating material (porous matrix) which greatly prevents heat loss and accelerates the process of cooling/heating as the case may be serving as a heat exchanger.
- (ii) Consideration of mass diffusion as the flow of industrial fluids is subjected to more than one fluid either generated/provided externally.
- (iii) Inclusion of chemical reaction term in the mass transport equation which is vital since the fluids may be chemically reactive.

The present study is a generalized approach by which we can discuss the results of Chen [18] as a special case, without considering mass diffusion and porous medium. Moreover, it is intended to bring out the effects of the emerging parameters on the heat and mass transport phenomena. The confluent hyper-geometric function i.e. Kummer's function has been used to solve the heat and mass transport equations after using similarity transformation which reduces the governing partial differential equations into ordinary differential equations.

## 2. Formulation of the problem

Consider a steady two-dimensional boundary-layer flow of an electrically conducting, viscoelastic fluid past a stretching sheet embedded in a porous medium, the flow being confined to  $y > 0$ . Two equal and opposite forces are applied along  $x$ -axis so that the surface is stretched, keeping the origin fixed. Assuming that a uniform magnetic field of strength  $B_0$  is applied along  $y$ -axis that generates magnetic effect in the  $x$ -direction. Under the usual boundary layer assumptions, the equations of continuity, momentum, energy and species concentration for the flow of viscoelastic fluid are:

$$\frac{\partial u}{\partial x} + \frac{\partial v}{\partial y} = 0 \quad (1)$$

$$u \frac{\partial u}{\partial x} + v \frac{\partial u}{\partial y} = \nu \frac{\partial^2 u}{\partial y^2} + \frac{k_0}{\rho} \left( \frac{\partial}{\partial x} \left( u \frac{\partial^2 u}{\partial y^2} \right) + \nu \frac{\partial^3 u}{\partial y^3} + \frac{\partial u}{\partial y} \frac{\partial^2 u}{\partial x \partial y} \right) - \frac{\sigma B_0^2 u}{\rho} - \frac{\nu u}{K_p} \quad (2)$$

$$\begin{aligned} \rho C_p \left( u \frac{\partial T}{\partial x} + v \frac{\partial T}{\partial y} \right) &= k \frac{\partial^2 T}{\partial y^2} + \mu \left( \frac{\partial u}{\partial y} \right)^2 \\ &+ k_0 \left( \frac{\partial u}{\partial y} \frac{\partial}{\partial y} \left( u \frac{\partial u}{\partial x} + v \frac{\partial u}{\partial y} \right) \right) \\ &+ \sigma B_0^2 u^2 - \frac{\partial q_r}{\partial y} + q(T - T_\infty) \end{aligned} \quad (3)$$

$$u \frac{\partial C}{\partial x} + v \frac{\partial C}{\partial y} = D \frac{\partial^2 C}{\partial y^2} - K'_c (C - C_\infty) \quad (4)$$

Rosseland's approximation for thermal radiation gives  $q_r = -\frac{4\sigma^*}{3k_1} \frac{\partial(T^4)}{\partial y}$ . It is assumed that the temperature variation within the flow is such that  $T^4$  may be expanded in a Taylor series. Expanding  $T^4$  about  $T_\infty$  and neglecting the higher order terms, we have

$$T^4 = 4T_\infty^3 T - 3T_\infty^4$$

and

$$\frac{\partial q_r}{\partial y} = -\frac{16\sigma^* T_\infty^3}{3k_1 \rho C_p} \frac{\partial^2 T}{\partial y^2}.$$

Substituting the above value of  $\frac{\partial q_r}{\partial y}$  in Eq. (3), we get

$$\begin{aligned} u \frac{\partial T}{\partial x} + v \frac{\partial T}{\partial y} &= \alpha \frac{\partial^2 T}{\partial y^2} + \frac{\mu}{\rho C_p} \left( \frac{\partial u}{\partial y} \right)^2 \\ &+ \frac{k_0}{\rho C_p} \left( \frac{\partial u}{\partial y} \frac{\partial}{\partial y} \left( u \frac{\partial u}{\partial x} + v \frac{\partial u}{\partial y} \right) \right) \\ &+ \frac{16\sigma^* T_\infty^3}{3k_1 \rho C_p} \frac{\partial^2 T}{\partial y^2} + \frac{q}{\rho C_p} (T - T_\infty) + \frac{\sigma B_0^2}{\rho C_p} u^2 \end{aligned} \quad (5)$$

The boundary conditions are:

$$\left. \begin{aligned} u &= u_w = Ex, \quad v = v_w, \quad T = T_w(x) = T_\infty + A \left( \frac{x}{L} \right)^2 && \text{(PST case),} \\ h_w(x) &= -k \left( \frac{\partial T}{\partial y} \right) = B \left( \frac{x}{L} \right)^2 && \text{(PHF case),} \\ C &= C_w(x) = C_\infty + E_0 \left( \frac{x}{L} \right)^2, \quad m_w = -D \left( \frac{\partial C}{\partial y} \right) = E_1 x^2, && \text{at } y \rightarrow 0 \\ u &= 0, \quad \frac{\partial u}{\partial y} = 0, \quad T \rightarrow T_\infty, \quad C \rightarrow C_\infty, && \text{at } y \rightarrow \infty \end{aligned} \right\} \quad (6)$$

## 3. Solution of the flow field

Eqs. (1) and (2) admit self-similar solutions of the form

$$f = \frac{\psi}{\nu \sqrt{Re_x}}, \quad \eta = \frac{y}{x} \sqrt{Re_x} \quad (7)$$

where  $f$  is the dimensionless stream function and  $\eta$  is the similarity variable and  $Re_x = u_w x / \nu$  is the local Reynolds number,  $\psi(x, y)$  is the stream function satisfying the continuity Eq. (1).

Substituting Eq. (7) in Eq. (2), we get

$$\begin{aligned} f''' + ff'' - (f')^2 + R_c \{ 2f'f'' - (f'')^2 - ff^{iv} \} \\ - \left( M_n + \frac{1}{K_p} \right) f' = 0 \end{aligned} \quad (8)$$

where  $R_c = k_0 E / \mu$  is the viscoelastic parameter,  $M_n = \sigma B_0^2 / \rho E$  is the magnetic parameter and  $K_p = \frac{EK'_p}{\nu}$  is the non-dimensional permeability parameter.

The corresponding boundary conditions are:

$$f(0) = f_w, \quad f'(0) = 1, \quad f'(\infty) = 0, \quad f''(\infty) = 0 \quad (9)$$

where  $f_w = \frac{-v_w \sqrt{Re_x}}{u_w}$  is the suction/injection parameter,  $f_w > 0$  and  $f_w < 0$  represent suction and injection respectively.

The exact solution of Eq. (8) with boundary conditions expressed in Eq. (9) following Chakrabati and Gupta [19] is in the form

$$f(\eta) = \frac{1 - e^{-r\eta}}{r} + f_w, \quad (10)$$

where  $r$  is a real positive root of the cubic algebraic equation

$$R_c f_w r^3 + (R_c + 1)r^2 - f_w r - \left(1 + M_n + \frac{1}{K_p}\right) = 0 \quad (11)$$

The velocity profile can be obtained from Eq. (10) as

$$f'(\eta) = e^{-r\eta} \quad (12)$$

The shear stress at the wall is defined as

$$\tau_w = \mu \left( \frac{\partial u}{\partial y} \right)_{y=0} = \mu Ex \sqrt{E/v} f''(0) \quad (13)$$

The non-dimensional form of skin friction coefficient at the wall is

$$C_f Re_x^{1/2} = -f''(0) = r \quad (14)$$

## 4. Heat transfer analysis

### 4.1. Case I: prescribed surface temperature (PST)

In prescribed surface temperature case, introducing non-dimensional quantities  $\theta(\eta) = \frac{T - T_\infty}{T_w - T_\infty}$ ,  $Pr = v/\alpha$ ,  $Ec = \frac{E^2 l^2}{AC_p}$ ,  $R_c = \frac{Ek_0}{\mu}$ ,  $Q = \frac{q}{E\rho C_p}$ ,  $R = \frac{16\sigma^* T_\infty^3}{3k_1 k}$  and using Eq. (6), Eq. (5) becomes

$$(1+R)\theta'' + Prf\theta' + Pr(Q - 2f')\theta = -EcPr \left( (f'')^2 + R_c(f'f'' - ff'') \right) + \left( M_n + \frac{1}{K_p} \right) (f')^2 \quad (15)$$

with the boundary conditions

$$\theta(0) = 1, \quad \theta(\infty) = 0 \quad (16)$$

Introducing the variable  $\xi = -\frac{Pr e^{-r\eta}}{(1+R)r^2}$ , Eq. (15) transformed to

$$\xi \frac{d^2 \theta}{d\xi^2} + \left( 1 - \frac{PrS}{(1+R)r^2} - \xi \right) \frac{d\theta}{d\xi} + \left( \frac{PrQ}{(1+R)r^2 \xi} + 2 \right) \theta = -\frac{Ec(1+R)r^4}{Pr} \left[ 1 + R_c S + \frac{1}{r^2} \left( M_n + \frac{1}{K_p} \right) \right] \xi \quad (17)$$

with the boundary conditions

$$\theta \left( \xi = -\frac{Pr}{(1+R)r^2} \right) = 1, \quad \theta(\xi = 0) = 0 \quad (18)$$

where  $S = 1 + rf_w$ .

Using confluent hypergeometric function of first kind (Kummer's function), we get,

$$\begin{aligned} \theta(\xi) = & \left[ 1 + \frac{EcPr \left\{ 1 + R_c S + \frac{1}{r^2} \left( M_n + \frac{1}{K_p} \right) \right\}}{(1+R)\{4 - (2S - Q)Pr^*\}} \right] \\ & \times \left( \frac{\xi}{-Pr^*} \right)^a \frac{M(a-2, b+1; \xi)}{M(a-2, b+1; -Pr^*)} \\ & - \frac{EcPr \left\{ 1 + R_c S + \frac{1}{r^2} \left( M_n + \frac{1}{K_p} \right) \right\}}{(1+R)\{4 - (2S - Q)Pr^*\}} \left( \frac{\xi}{Pr^*} \right)^2 \end{aligned} \quad (19)$$

where,

$$a = \frac{Pr^* S + \sqrt{(Pr^* S)^2 - 4Pr^* Q}}{2},$$

$$b = \sqrt{(Pr^* S)^2 - 4Pr^* Q}, \quad Pr^* = \frac{Pr}{(1+R)r^2}, \quad S = 1 + rf_w$$

and  $M(\alpha_1, \alpha_2; x)$  denotes the Kummer's function and is given by

$$M(\alpha_1, \alpha_2; x) = \sum_{n=0}^{\infty} \frac{(\alpha_1)_n x^n}{(\alpha_2)_n n!}, \quad \alpha_2 \neq 0, -1, -2, \dots \quad (20)$$

where  $(\alpha)_n$  denoting the Pochhammer symbol defined in terms of the gamma function as

$$(\alpha)_n = \alpha(\alpha+1)(\alpha+2)\dots(\alpha+n-1) = \frac{\Gamma(\alpha+n)}{\Gamma(\alpha)} \quad (21)$$

The temperature profile in terms of  $\eta$  can be written as

$$\begin{aligned} \theta(\eta) = & \left[ 1 + \frac{EcPr \left\{ 1 + R_c S + \frac{1}{r^2} \left( M_n + \frac{1}{K_p} \right) \right\}}{(1+R)\{4 - (2S - Q)Pr^*\}} \right] \\ & \times e^{-ar\eta} \frac{M(a-2, b+1; -Pr^* e^{-r\eta})}{M(a-2, b+1; -Pr^*)} \\ & - \frac{EcPr \left\{ 1 + R_c S + \frac{1}{r^2} \left( M_n + \frac{1}{K_p} \right) \right\}}{(1+R)\{4 - (2S - Q)Pr^*\}} e^{-2r\eta} \end{aligned} \quad (22)$$

The dimensionless wall temperature gradient is given by

$$\begin{aligned} \theta'(0) = & r \left[ 1 + \frac{EcPr \left\{ 1 + R_c S + \frac{1}{r^2} \left( M_n + \frac{1}{K_p} \right) \right\}}{(1+R)\{4 - (2S - Q)Pr^*\}} \right] \\ & \left[ Pr^* \left( \frac{a-2}{b+1} \right) \frac{M(a-1, b+2; -Pr^*)}{M(a-2, b+1; -Pr^*)} - a \right] \\ & + 2r \left[ \frac{EcPr \left\{ 1 + R_c S + \frac{1}{r^2} \left( M_n + \frac{1}{K_p} \right) \right\}}{(1+R)\{4 - (2S - Q)Pr^*\}} \right] \end{aligned} \quad (23)$$

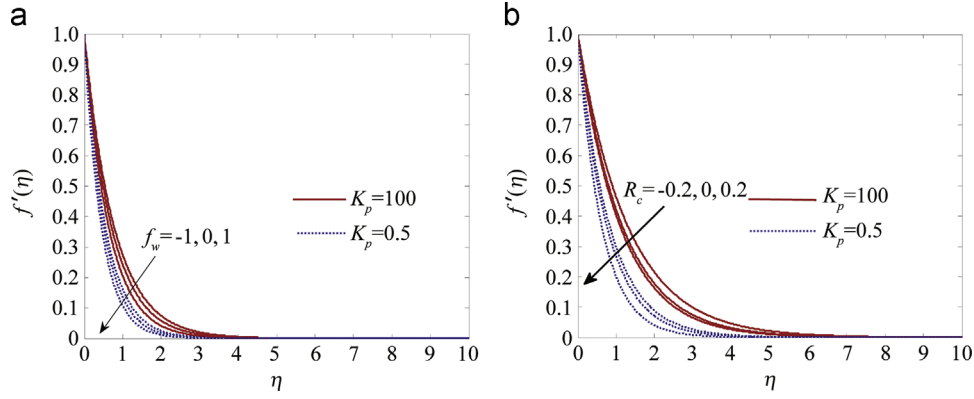


**Figure 1** (a) Velocity profiles (second grade fluid) for  $M_n = 0.5$ ,  $R_c = 1$  and (b) velocity profiles for  $M_n = 1$ ,  $f_w = 0$ .

The local Nusselt number for PST case is

$$Nu_x Re_x^{-1/2} = -\theta'(0) \quad (24)$$

#### 4.2. Case II: prescribed heat flux (PHF)

In prescribed heat flux case, introducing the similarity variable  $T - T_\infty = \frac{Bx^2}{kL^2} \sqrt{\frac{v}{E}} \psi(\eta)$  and using Eq. (6), Eq. (5) becomes

$$(1+R)\psi'' + Prf\psi' + Pr(Q - 2f')\psi = -EcPr \left[ (f'')^2 + R_c f''(f'f'' - ff''') + \left(M_n + \frac{1}{K_p}\right)(f')^2 \right] \quad (25)$$

with the boundary conditions

$$\psi(0) = -1, \quad \psi(\infty) = 0 \quad (26)$$

where  $Ec = \frac{E^2 L^2 k \sqrt{E/v}}{BC_p}$  is the Eckert number and the other parameters are as defined in the PST case.

Substituting  $\xi = -\frac{Pre^{-\eta}}{(1+R)r^2}$  in Eqs. (25) and (26), we get respectively

$$\xi \frac{d^2 \psi}{d\xi^2} + \left(1 - \frac{PrS}{(1+R)r^2} - \xi\right) \frac{d\psi}{d\xi} + \left(\frac{PrQ}{(1+R)r^2 \xi} + 2\right) \psi = -\frac{Ec(1+R)r^4}{Pr} \left[1 + R_c S + \frac{1}{r^2} \left(M_n + \frac{1}{K_p}\right)\right] \xi \quad (27)$$

$$\psi(\xi = 0) = 0, \quad \psi' \left( \xi = -\frac{Pr}{(1+R)r^2} \right) = -\frac{(1+R)r}{Pr} \quad (28)$$

The exact solution of Eq. (27) subject to the boundary conditions expressed in Eq. (28) can be written in terms of confluent hypergeometric function in terms of similarity variable  $\eta$  and is given by

$$\begin{aligned} \psi(\eta) = & \left[ \frac{1}{r} + 2 \left[ \frac{EcPr \left\{ 1 + R_c S + \frac{1}{r^2} \left( M_n + \frac{1}{K_p} \right) \right\}}{(1+R)\{4 - (2S - Q)Pr^*\}} \right] \right] e^{-a\eta} M(a-2, b+1; -Pr^* e^{-\eta}) \\ & - \frac{aM(a-2, b+1; -Pr^*) - Pr^* \left( \frac{a-2}{b+1} \right) M(a-1, b+2; -Pr^*)}{aM(a-2, b+1; -Pr^*) - Pr^* \left( \frac{a-2}{b+1} \right) M(a-1, b+2; -Pr^*)} \\ & - \left[ \frac{EcPr \left\{ 1 + R_c S + \frac{1}{r^2} \left( M_n + \frac{1}{K_p} \right) \right\}}{(1+R)\{4 - (2S - Q)Pr^*\}} \right] e^{-2r\eta} \end{aligned} \quad (29)$$

The dimensionless wall temperature can be expressed as

$$\begin{aligned} \psi(\eta) = & \frac{\frac{1}{r} + 2 \left[ \frac{EcPr \left\{ 1 + R_c S + \frac{1}{r^2} \left( M_n + \frac{1}{K_p} \right) \right\}}{(1+R)\{4 - (2S - Q)Pr^*\}} \right] M(a-2, b+1; -Pr^*)}{aM(a-2, b+1; -Pr^*) - Pr^* \left( \frac{a-2}{b+1} \right) M(a-2, b+2; -Pr^*)} \\ & - \left[ \frac{EcPr \left\{ 1 + R_c S + \frac{1}{r^2} \left( M_n + \frac{1}{K_p} \right) \right\}}{(1+R)\{4 - (2S - Q)Pr^*\}} \right] \end{aligned} \quad (30)$$

The local Nusselt number for the PHF case can be written as

$$Nu_x Re_x^{-1/2} = \frac{1}{\psi(0)} \quad (31)$$

## 5. Mass transfer analysis

Introducing the similarity variable  $C - C_\infty = \frac{E_1 x^2}{D} \sqrt{\frac{v}{E}} \phi(\eta)$  and using Eq. (6) in Eq. (4),

$$\phi'' + Scf\phi' - Scf'\phi - ScK_c\phi = 0 \quad (32)$$

with the boundary conditions

$$\begin{aligned} \phi' &= -1 \quad \text{at } \eta = 0 \\ \phi &\rightarrow 0 \quad \text{at } \eta \rightarrow \infty \end{aligned} \quad (33)$$

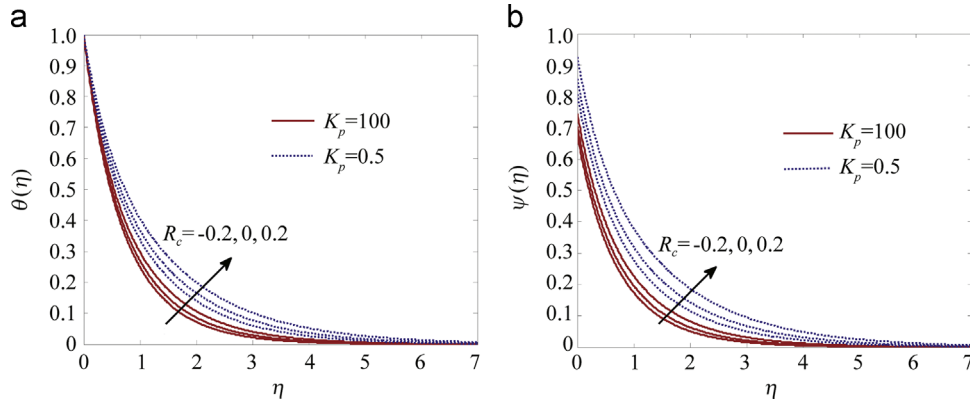


**Figure 2** (a) Temperature profiles for  $Pr=3$ ,  $M_n=1$ ,  $Ec=0.1$ ,  $R=1$ ,  $Q=0$ ,  $f_w=0$  (PST case) and (b) temperature profiles for  $Pr=3$ ,  $M_n=1$ ,  $Ec=0.1$ ,  $R=1$ ,  $Q=0$ ,  $f_w=0$  (PHF case).

Again introducing a new variable  $\xi = -\frac{Sc}{r^2}e^{-r\eta}$ , Eq. (32) becomes

$$\xi \frac{d^2\phi}{d\xi^2} + \left[ \left( 1 - \frac{Sc}{r^2} \left( r^2 - M_n - \frac{1}{K_p} \right) \right) - \xi \right] \frac{d\phi}{d\xi} + \left( 2 - \frac{K_c}{r^2\xi} \right) \phi = 0 \quad (34)$$

The corresponding boundary conditions are

$$\begin{aligned} \phi(\xi=0) &= 0, \\ \phi' \left( \xi = -\frac{Sc}{r^2} \right) &= -\frac{r}{Sc} \end{aligned} \quad (35)$$

The exact solution of Eq. (34) subject to the boundary condition expressed in Eq. (35) is given by

$$\phi(\eta) = \frac{e^{-\left(\frac{S_1+S_2}{2}\right)r\eta} M\left(\frac{S_1+S_2-4}{2}, 1+S_1; -\frac{Sc}{r^2}e^{-r\eta}\right)}{\frac{r(S_1+S_2)}{2} M\left(\frac{S_1+S_2-4}{2}, 1+S_1; -\frac{Sc}{r^2}\right) - \frac{Sc}{r} \left[ \left( \frac{S_1+S_2-2}{2(1+S_1)} \right) M\left(\frac{S_1+S_2-2}{2}, 2+S_1; -\frac{Sc}{r^2}\right) \right]} \quad (36)$$

where  $S_1 = \frac{Sc}{r^2} \left[ r^2 - \left( M^2 + \frac{1}{K_p} \right) \right]$  and  $S_2 = \sqrt{S_1^2 + \frac{4K_c}{r^2}}$ .

The dimensionless wall concentration gradient is given by

$$\phi'(0) = \frac{-r \left( \frac{S_1+S_2}{2} \right) M\left(\frac{S_1+S_2-4}{2}, 1+S_1; -\frac{Sc}{r^2}e^{-r\eta}\right) + M\left(\frac{S_1+S_2-2}{2}, 2+S_1; -\frac{Sc}{r^2}e^{-r\eta}\right)}{\frac{r(S_1+S_2)}{2} M\left(\frac{S_1+S_2-4}{2}, 1+S_1; -\frac{Sc}{r^2}\right) - \frac{Sc}{r} \left[ \left( \frac{S_1+S_2-2}{2(1+S_1)} \right) M\left(\frac{S_1+S_2-2}{2}, 2+S_1; -\frac{Sc}{r^2}\right) \right]} \quad (37)$$

The local Sherwood number can be expressed as

$$S_{hx} Re_x^{-1/2} = -\phi'(0) \quad (38)$$

## 6. Analysis of physical exponential solutions

We can analyze the constraints imposed on the viscoelasticity parameter and magnetic parameter so that the existence/non-existence of single/double solutions of purely exponential type for the system (Eqs. (8) and (9)) can be obtained following Turkyilmazoglu [20,21].

## 7. Results and discussion

In the course of discussion the following aspects are highlighted.

- (i) Effect of permeability of the medium on flow characteristics.
- (ii) Effect of diffusion species as well as first order chemical reaction.
- (iii) Relative response of two viscoelastic models to

velocity and temperature distribution in the presence of uniform porous matrix.

- (iv) Presenting the generality of the present study by discussing the previous result as particular case.

It is important to note that  $R_c > 0$ ,  $R_c < 0$  and  $R_c = 0$  represent second grade, Walters  $B'$  and viscous fluids respectively.



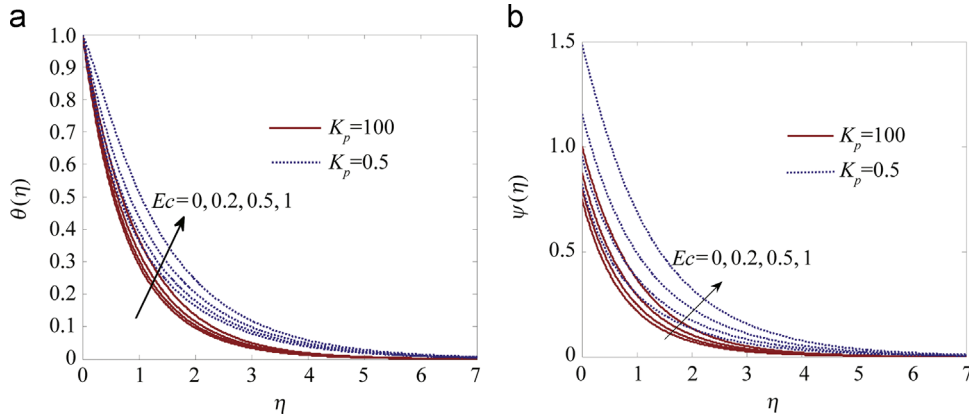


**Figure 3** (a) Temperature profiles for  $Pr=1$ ,  $M_n=1$ ,  $R_c=1$ ,  $R=0$ ,  $Q=0$ ,  $f_w=0$  (PST case) and (b) temperature profiles for  $Pr=3$ ,  $M_n=1$ ,  $Ec=0.1$ ,  $R_c=1$ ,  $R=0$ ,  $Q=0$ ,  $f_w=0$  (PHF case).

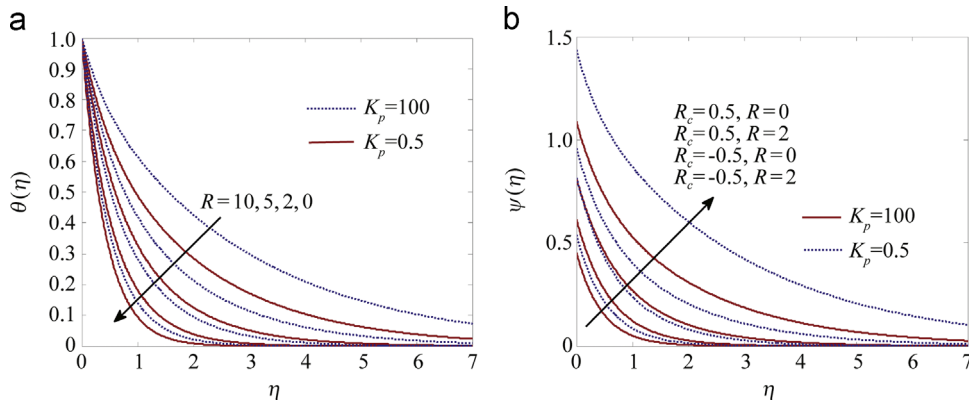


**Figure 4** (a) Temperature profiles for  $Pr=3$ ,  $M_n=1$ ,  $Ec=0.1$ ,  $R_c=0.5$ ,  $Q=0$ ,  $f_w=0$  (PST case) and (b) temperature profiles for  $Pr=3$ ,  $M_n=1$ ,  $Ec=0.1$ ,  $Q=0$ ,  $f_w=0$  (PHF case).

Figure 1(a) shows the velocity distribution of second grade fluid for suction ( $f_w > 0$ ), injection ( $f_w < 0$ ) and impermeable plate ( $f_w = 0$ ) in the presence ( $K_p = 0.5$ ) and absence ( $K_p = 100$ ) of porous matrix. The profiles  $K_p = 100$ ,  $M_n = 0.5$ ,  $R_c = 1$  coincide with Figure 1(b) of Chen [18] and hence our result finds a good agreement. The porous medium ( $K_p = 0.5$ ) reduces the primary velocity at all points due to resistive force offered by the porous medium which results in thinning of boundary layer. Further, it is interesting to note that the suction at the plate reduces the velocity. Thus, it is concluded that combined effect of suction and porous matrix favorable to thinning of boundary layer which favors the stability of the flow.

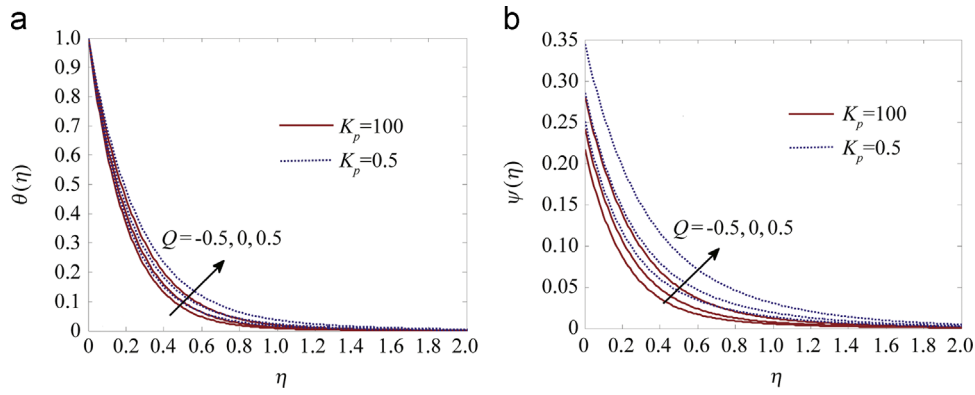
Figure 1(b) exhibits the velocity profiles for Walters  $B'$  ( $R_c = -0.2$ ), viscous ( $R_c = 0$ ) and second grade flow ( $R_c = 0.2$ ). It is observed that velocity attains low value in case of visco-elasticity (Walters  $B'$  model), in the presence of porous medium. Viscoelastic flows are prone to instabilities due to non-linearity in the constitutive equations. Instabilities are mainly driven by the fluid normal stresses (elasticity) or by the nature of the boundary conditions. Therefore, elastic property of Walters flow model in conjunction with the permeability of the porous medium

reduces the boundary layer thickness and hence reduces the instability.

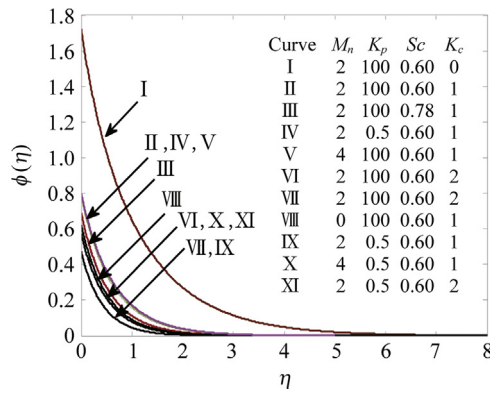
Figure 2(a) and (b) displays the temperature distribution in case of PST and PHF cases respectively without suction/injection. The effects of the permeability of the medium and elasticity of the fluid subject to present study on temperature distribution are opposite to that of viscous dissipation that is the temperature increases at all points and this is further contributed by Walters  $B'$  model. Both the cases of PST and PHF display the same effect.

Figure 3(a) and (b) illustrate the effects of Eckert number in case of second grade fluid in the absence of suction/injection and thermal radiation in both PST and PHF cases. The energy dissipation of the flow configuration is measured by Eckert number. It is seen that an increase in  $Ec$  increases the temperature and hence increases the thermal boundary layer thickness. This leads to reduction of the rate of heat transfer from the plate surface. This reduction is further decreased due to presence of porous medium. Therefore, the presence of porous medium acts as an insulator to the plate surface. This result is in good agreement with the result of Chen [18].

Figure 4(a) and (b) delineate the effect of radiation parameter in case of second grade fluid. It is observed that



**Figure 5** (a) Temperature profiles for  $Pr=3$ ,  $M_n=1$ ,  $Ec=0.1$ ,  $R_c=0.5$ ,  $R=0$ ,  $f_w=0.5$  (PST case) and (b) temperature profiles for  $Pr=3$ ,  $M_n=1$ ,  $Ec=0.1$ ,  $R_c=0.5$ ,  $R=0$ ,  $f_w=0.5$  (PHF case).



**Figure 6** Concentration profiles.

an increase in thermal radiation parameter ( $R$ ) increases the temperature of the fluid layer and the processes get accelerated due to the presence of the porous matrix. The increase in temperature with an increase in radiation parameter causes a reduction in temperature gradient of the wall in PST case. Thus, it is concluded that thermal radiation is to reduce in order to make the cooling process faster.

Figure 5(a) and (b) exhibit the effect of the internal heat generation/absorption parameter ( $Q$ ) on the temperature distribution  $\theta(\eta)$  (PST) and  $\psi(\eta)$  (PHF) in case of second grade fluid. This shows that an increase in heat source strength ( $Q>0$ ) increases the temperature. This is due to generation of the heat in thermal boundary layer which causes the temperature to rise. In similar manner the heat sink causes the temperature absorption resulting in decrease in temperature. The result holds good for both PST and PHF. The role of porous matrix is to accelerate/decelerate the process in case of source/sink respectively.

Figure 6 exhibits the concentration profiles for various values of the parameters characterizing the concentration distribution. It is observed that chemical reaction parameter reduces the concentration distribution at all points irrespective of the presence or absence of porous matrix. From the curves V and X it is seen that the presence of porous matrix enhances the concentration level at all points of the flow

**Table 1** Skin friction coefficients.

$M_n$	$K_p$	$R_c$	$\tau$ ( $f_w=0$ )	$\tau$ ( $f_w=1$ )
1	<b>100</b>	−0.5	−2.00499	<b>1.002852</b>
1	<b>0.5</b>	−0.5	−2.82843	<b>1.445428</b>
0.5	<b>100</b>	−0.5	−1.73781	<b>0.847162</b>
0.5	<b>0.5</b>	−0.5	−2.64575	<b>1.351683</b>
1	<b>100</b>	0.5	−1.15758	<b>1.004</b>
1	<b>0.5</b>	0.5	−1.63299	<b>2</b>
0.5	<b>100</b>	0.5	−1.00333	<b>0.802458</b>
0.5	<b>0.5</b>	0.5	−1.52753	<b>1.65662</b>
1	<b>100</b>	1.0	−1.0025	<b>1.005013</b>
1	<b>0.5</b>	1.0	−1.41421	<b>−1.26953</b>
0.5	<b>100</b>	1.0	−0.86891	<b>0.774667</b>
0.5	<b>0.5</b>	1.0	−1.32288	<b>−1.21124</b>

domain in the presence of chemical reaction. Now, it is further seen that the effect of magnetic field is to increase the concentration (Curve II,  $M=2$ , Curve VII,  $M=0$ ) but further increase in  $M$  has no significant effect on concentration field in the absence of porous matrix whereas in the presence of porous matrix (Curves IV and IX) an increase in magnetic field reduces the concentration level. Moreover, heavier species (high value of  $Sc$ ) contributes to the reduction in the level of concentration in the absence of porous matrix (Curves II and III).

From Table 1 it is noticed that an increasing magnetic parameter enhances the skin friction and it is further increased due to the presence of porous matrix. However, elasticity effect increases the skin friction. Thus, it is concluded that higher values of elastic elements are favorable in enhancing the skin friction in both impermeable ( $f_w=0$ ) and permeable ( $f_w \neq 0$ ) surfaces.

Tables 2 and 3 show the comparison of temperature gradients for second grade and second order fluids in PST and PHF cases respectively. On comparison it is observed that the results accomplished by Liu [22] and Datti [23] well agree with the present study. From Table 2, it is seen that the absence of porous matrix and magnetic parameter with higher Prandtl value cause the Nusselt number to increase irrespective of source/sink in PST whereas, the



**Table 2** Comparison of Nusselt numbers to Liu [22] for a second-grade fluid for  $R_c=1.0$ ,  $Ec=0.2$ ,  $R=0$  and  $f_w=0$ .

$M_n$	$K_p$	$Q$	$Pr$	PST case		PHF case	
				Liu [22]	Present case	Liu [22]	Present case
0.0	100	-0.1	1	1.37488	1.372608	0.742096	0.7435
	100	-0.1	10	4.59962	4.591724	0.276367	0.277832
	0.5	-0.1	1		1.032946		0.975079
	0.5	-0.1	10		3.249158		0.536112
	100	0	1	1.337265	1.331574	0.764213	0.765383
	100	0	10	4.48696	4.478859	0.284146	0.28568
	0.5	0	1		0.974733		1.019901
	0.5	0	10		3.103711		0.55611
	100	0.1	1	1.29111	1.288637	0.788006	0.789645
	100	0.1	10	4.37115	4.362827	0.292579	0.294189
	0.5	0.1	1		0.906795		1.077075
	0.5	0.1	10		2.952014		0.578134
	100	-0.1	1	1.18298	1.181325	0.876313	0.868455
	100	-0.1	10	3.87868	3.87202	0.412923	0.414209
1.0	0.5	-0.1	1		0.906259		1.073528
	0.5	-0.1	10		2.676623		0.65084
	100	0	1	1.13333	1.131589	0.9	0.901256
	100	0	10	3.74805	3.741224	0.427117	0.428464
	0.5	0	1		0.839487		1.132026
	0.5	0	10		2.518129		0.67632
	100	0.1	1	1.0792	1.077335	0.938308	0.939725
	100	0.1	10	3.61261	3.605617	0.442665	0.444078
	0.5	0.1	1		0.75274		1.216857
	0.5	0.1	10		2.352002		0.704501

**Table 3** Comparison of Nusselt numbers to Datti et al. [23] for Walters' liquid  $B'$ .

$Pr$	$R_c$	$M_n$	$K_p$	$Q$	$R$	PST case		PHF case	
						Datti et al. [23]	Present case	Datti et al. [23]	Present case
1	0	0	100	0	0	1.3333	1.331932		0.750789
1	0	0	100	-0.1	0		1.377796	0.7251	0.725797
1	0	0	0.5	0	0		1.126898		0.887391
1	0	0	0.5	-0.1	0		1.199394		0.833755
1	0	1	100	0	0	1.2158	1.214771		0.823201
1	0	1	100	-0.1	0		1.274028	0.7843	0.784912
1	0	1	0.5	0	0		1.055361		0.947543
1	0	1	0.5	-0.1	0		1.140395		0.876889
1	-0.1	0.1	100	-0.1	0	1.3521	1.350924	0.7395	0.740234
1	-0.1	0.1	100	0	0	1.3035	1.302129	0.7671	0.767973
1	-0.1	0.1	100	0.1	0	1.2496	1.247923	0.8002	0.801332
1	-0.1	0.1	0.5	-0.1	0		1.17154		0.853577
1	-0.1	0.1	0.5	0	0		1.093343		0.914626
1	-0.1	0.1	0.5	0.1	0		0.971376		1.026597
1	-0.1	0.1	100	-0.1	1	0.8812	0.874755	1.1348	1.143177
1	-0.1	0.1	0.5	-0.1	1		0.722385		1.384303
2	-0.1	0.1	100	-0.1	0	2.021	2.027636	0.4928	0.493185
2	-0.1	0.1	0.5	-0.1	0		1.17154		0.853577
3	-0.1	0.1	100	-0.1	0	2.5326	2.546397	0.3926	0.392712
3	-0.1	0.1	0.5	-0.1	0		2.357059		0.424257

reverse effect is attained in PHF. It is also seen that in the presence of porous matrix, the reverse trend appears in both PST and PHF. It is interesting to mention that in the presence of magnetic parameter with higher Prandtl value, the Nusselt number decreases in PST and increases in PHF

in presence/absence of porous matrix and source/sink. Thus, it is concluded that for second grade fluid, the characteristics of Nusselt number are achieved in the permeable surface ( $f_w = 0$ ) without thermal radiation ( $R = 0$ ). From Table 3 it is observed that absence of porous matrix with

**Table 4** Sherwood number.

$M_n$	$K_p$	$Sc$	$K_c$	$S_h$
3	100	0.6	0	1.331674
3	100	0.6	1	−1.90499
3	0.5	0.6	1	−2.35153
4	100	0.6	1	−2.14054
3	100	0.78	1	−1.90499
3	100	0.6	2	−1.93499

high  $Pr$  enhances the Nusselt number in PST and reduces in PHF and the reverse effect is attained in the presence of the porous matrix but increasing value of magnetic parameter, presence/absence of source/sink parameter and thermal radiation parameter lead to the reverse effects in both PST and PHF. Therefore, the rate of heat transfer is influenced by the presence of porous matrix, magnetic parameter and thermal radiation parameter causes instability in the rate of heat transfer phenomena.

Table 4 enlists the numerical values of the rate of mass transfer at the plate. It is interesting to observe that absence of chemical reaction contributes to positive values whereas presence of it gives rise to negative values. It is noticed that an increase in magnetic parameter ( $M_n$ ), porosity parameter ( $K_p$ ) and Schmidt parameter ( $Sc$ ) (that is for heavier species) enhances the Sherwood number whereas increase in chemical reaction parameter decreases the Sherwood number.

## 8. Conclusion

1. Porous matrix acting as an insulator to the vertical surface prevents energy loss due to free convection which in turn enhances the velocity.
2. Presence of porous matrix and elasticity of the fluid overcomes the resistive force of magnetic field and hence the velocity increases due to the presence of both.
3. Presence of elasticity also leads to increase the temperature at all points irrespective of presence/absence of porous matrix.
4. The slow rate of thermal diffusion in presence of magnetic field and porous matrix causes thinning of thermal boundary layer thickness.
5. The variation in temperature is more sensitive on account of heat flux.
6. Presence of chemical reaction as well as porous matrix with moderate values of magnetic parameter in case of heavier species reduces the concentration level.
7. Higher value of magnetic field in conjunction with porous matrix reduce the concentration level.
8. Presence of elastic element favors in reducing the skin friction in both permeable and impermeable surfaces.
9. Presence of magnetic parameter causes to decrease the Nusselt number in PST case and increase the same in PHF case

10. Presence of porous matrix and magnetic parameter influences the rate of heat transfer.
11. Porous matrix enhances the rate of mass transfer whereas increase in chemical reaction has no impact on the absence of porous matrix.

## References

- [1] B.C. Sakiadis, Boundary layer behavior on continuous solid surface, I: boundary-layer equations for two dimensional and axisymmetric flow, *AIChE J.* 7 (1) (1961) 26–28 221–235.
- [2] L.J. Crane, Flow past a stretching plane, *Z. Angew. Math. Phys.* 21 (4) (1970) 645–647.
- [3] S.K. Khan, E. Sanjayanand, Viscoelastic boundary layer flow and heat transfer over an exponential stretching sheet, *Int. J. Heat Mass Transf.* 48 (2005) 1534–1542.
- [4] M. Kar, S.N. Sahoo, P.K. Rath, G.C. Rath, Heat and mass transfer effects on a dissipative and radiative viscoelastic MHD flow over a stretching porous sheet, *Arab. J. Sci. Eng.* 39 (5) (2014) 3393–3401.
- [5] M. Mushtaq, S. Asghar, M.A. Hossain, Mixed convection flow of second grade fluid along a vertical stretching flat surface with variable surface temperature, *Heat Mass Transf.* 43 (2007) 1049–1061.
- [6] J.C. Arnold, A.A. Asir, S. Somasundaram, T. Christopher, Heat transfer in a viscoelastic boundary layer flow over a stretching sheet, *Int. J. Heat Mass Transf.* 53 (2010) 1112–1118.
- [7] R.C. Bataller, Viscoelastic fluid flow and heat transfer over a stretching sheet under the effects of a non-uniform heat source, viscous dissipation and thermal radiation, *Int. J. Heat Mass Transf.* 50 (2007) 3152–3162.
- [8] T. Hayat, M. Awais, A. Safdar, A.A. Hendi, Unsteady three dimensional flow of couple stress fluid over a stretching surface with chemical reaction, *Non-Linear Anal.: Model. Control* 17 (2012) 47–59.
- [9] B.J. Gireesha, A.J. Chamkha, S. Manjunatha, C.S. Bagewadi, Boundary-layer flow and heat transfer of a dusty fluid flow over a stretching sheet with non-uniform heat source/sink and radiation, *Int. J. Numer. Methods Heat Fluid Flow* 23 (4) (2013) 598–612.
- [10] A.B. Parsa, M.M. Rashidi, T. Hayat, MHD boundary-layer flow over a stretching surface with internal heat generation or absorption, *Heat Transf. Asian Res.* 42 (6) (2013) 500–514.
- [11] P.S. Gupta, A.S. Gupta, Heat and mass transfer on a stretching sheet with suction or blowing, *Can. J. Chem. Eng.* 55 (1977) 744–746.
- [12] K. Vajravelu, D. Rollins, Heat transfer in electrically conducting fluid over a stretching surface, *Int. J. Non-Linear Mech.* 27 (2) (1992) 265–277.
- [13] A. Raptis, Radiation and free convection flow through a porous medium, *Int. Commun. Heat Mass Transf.* 25 (1998) 289.
- [14] T.R. Mahapatra, A.S. Gupta, Stagnation-point flow of a visco-elastic fluid towards a stretching surface, *Int. J. Non-Linear Mech.* 39 (2004) 811.
- [15] R. Cortell, MHD flow and mass transfer of an electrically conducting fluid of second grade in a porous medium over a stretching sheet with chemically reactive species, *Chem. Eng. Process.* 46 (8) (2007) 721–728.

- [16] R. Cortell, Effect of viscous dissipation and radiation on the thermal boundary layer over a nonlinearly stretching sheet, *Phys. Lett. A* 372 (5) (2008) 631–636.
- [17] A.K. Singh, Heat source and radiation effects on magneto-convection flow of a viscoelastic fluid past a stretching sheet: analysis with Kummer's functions, *Int. Commun. Heat Mass Transf.* 35 (2008) 637–642.
- [18] C.H. Chen, On the analytic solution of MHD flow and heat transfer for two types of viscoelastic fluid over a stretching sheet with energy dissipation, internal heat source and thermal radiation, *Int. J. Heat Mass Transf.* 53 (2010) 4264–4273.
- [19] A. Chakrabarti, A.S. Gupta, Hydromagnetic flow and heat transfer over a stretching sheet, *Q. Appl. Math.* 37 (1979) 73–78.
- [20] M. Turkyilmazoglu, Dual and triple solutions for MHD slip flow of non-Newtonian fluid over a shrinking surface, *Comput. Fluids* 70 (2012) 53–58.
- [21] M. Turkyilmazoglu, Multiple solutions of heat and mass transfer of MHD slip flow for the viscoelastic fluid over a stretching sheet, *Int. J. Therm. Sci.* 50 (2011) 2264–2276.
- [22] I.C. Liu, Flow and heat transfer of an electrically conducting fluid of second grade over a stretching sheet subject to a transverse magnetic field, *Int. J. Heat Mass Transf.* 47 (2004) 4427–4437.
- [23] P.S. Datti, K.V. Prasad, M. Subash Abel, Ambuja Joshi, MHD viscoelastic fluid flow over a non-isothermal stretching sheet, *Int. J. Eng. Sci.* 42 (2004) 935–946.